Proceedings of *The Riddle of Cooling Flows in Galaxies and Clusters of Galaxies*: E4
May 31 – June 4, 2003, Charlottesville, Virginia, USA
Ed. T. H. Reiprich, J. C. Kempner, & N. Soker

Galaxy Clusters As Cosmological Tools and Astrophysical Laboratories

Stefano Borgani

Department of Astronomy, University of Trieste, via Tiepolo 11, I-34131 Trieste, Italy

In the first part of my contribution I discuss the role that X-ray galaxy clusters play in the determination of cosmological parameters. In particular I focus the discussion on the evolution of the cluster mass function for the determination of the density parameter Ω_m and the normalization of the power spectrum σ_8. Available constraints indicate that Ω_m lies in the range 0.2–0.5, with $\sigma_8 \simeq 0.7$–0.8 for $\Omega_m = 0.3$. I emphasize that the ability of clusters to provide such constraints is determined by the possibility of relating X-ray observable quantities to the cluster mass and, therefore, to our understanding of the physical processes taking place in the ICM. In this perspective, the second part of this contribution is devoted to the discussion of the relevance that hydrodynamical simulations of clusters can play to understand the ICM physics and to calibrate mass estimates from X-ray observable quantities. Using hydrodynamical simulations, which cover a quite large dynamical range and include a fairly advanced treatment of the gas physics (cooling, star formation and SN feedback), I show that scaling relations among X-ray observable quantities can be reproduced quite well. At the same time, these simulations fail at accounting for several observational quantities, which are related to the cooling structure of the ICM: the fraction of stars, the temperature profiles and the gas entropy in central cluster regions. This calls for the need of introducing in simulations suitable physical mechanisms which should regulate the cooling structure of the ICM.

1. Introduction

Clusters of galaxies probe the high-density tail of the cosmic density field and their number density is highly sensitive to specific cosmological scenarios (e.g., Press & Schechter 1974). The mass function of galaxy clusters and its evolution are currently used to measure the amplitude of density perturbations on $\sim$10 Mpc scales and to place constraints on the value of the matter density parameter Ω_m (e.g., Oukbir & Blanchard 1992; Eke et al. 1998; Borgani et al. 2001). In this way, probing the evolution of the population of galaxy clusters provides a sensitive probe of the cosmological scenario, which is intrinsically and conceptually complementary to that provided by observations of the CMB anisotropies (e.g., Spergel et al. 2003). However, what cosmological models predict is the number density of clusters of a given mass at varying redshifts. On the other hand, the cluster mass is never a directly observable quantity, although several methods exist to estimate it from observations.

The ROSAT All-Sky Survey and deep PSPC and HRI ROSAT pointings have offered during the last decade a unique means to compile extended samples of X-ray clusters from redshift $z \lesssim 0.1$, out to $z \simeq 1.3$, with well defined selection functions (see Rosati, Borgani & Norman 2002, for a recent review). While these samples have been already used to probe the evolution of the cluster population over a fairly large redshift baseline, forthcoming surveys based on XMM-Newton and Chandra data will further contribute to substantially enlarge the statistics of distant clusters. At the same time, large N-body simulations now allow to trace the gravitational evolution and the formation of dark-matter (DM) halos over a quite large dynamical range (e.g., Evrard et al. 2002). Such simulations have allowed to improve the original approach by Press & Schechter (1974) and to define precise universal fitting functions to describe the mass function of DM halos for different cosmological models (e.g., Sheth & Tormen 1999; Jenkins et al. 2001; White 2002).

As of today, the availability of robust relations between cluster masses and X-ray observable quantities represents the main source of uncertainty for using clusters as tools for precision cosmology. For instance, the X-ray luminosity, L_X, is highly sensitive to the details of the gas distribution, to the overall dynamical status of clusters and to the structure of their central cooling regions. At the same time, the presence of unresolved temperature profiles and/or local violation of the condition of hydrostatic equilibrium, may introduce significant uncertainties in the relation between temperature and the cluster mass M. This calls for the need of understanding in detail the physical processes, which are relevant for establishing the observational properties of clusters. Among such processes, radiative cooling and heating of the intracluster medium (ICM) from supernova and AGN are already known to play important roles in determining the thermodynamical properties of the gas and, therefore, its emissivity and temperature. In this respect, hydrodynamical simulations of clusters represent now invaluable tools to treat such complex physical processes and to shed light on the interplay between the cosmological framework, which defines the pattern of cluster formation, and the astrophysical processes, which determine the X-ray observational properties of the ICM.

A number of observational facts have now established that the thermodynamical properties of the ICM can not be determined by the influence of gravitational heating only. For instance, the slope of the L_X–T relation (e.g., Arnaud & Evrard 1999), the entropy level of the gas in the central regions of poor clusters and groups (e.g., Sanderson et al. 2003), and the amplitude of the M–T relation (e.g., Finoguenov et al. 2001) all show departures with respect to the prediction of the so-called self-similar model, which is based on gravitational processes only regulating the ICM thermal properties (Kaiser 1986).

Two alternative routes have been proposed to solve this discrepancy. The first possibility assumes that the diffuse gas underwent non-gravitational heating, possibly before the cluster collapse epoch, due to the action of some astrophysical source of energy feedback (e.g., SNe or AGN). The consequence of this heating is that of increasing its entropy and avoiding it from reaching high density during the DM halo collapse, thus suppressing its X-ray emissivity (Tozzi & Norman 2001). The second possibility assumes radiative cooling to be responsible for the lack of ICM self-similarity. Cooling acts in such a way to remove from the hot X-ray emitting phase the gas having low enough entropy that its cooling time, t_{cool}, is shorter than the cluster typical lifetime (e.g., Voit et al. 2002). In this case, the observed entropy excess is the consequence of the removal of low-entropy gas, while the suppressed L_X follows from the reduced amount of gas left in the diffuse phase. Both explanations have their pros and cons. While non-gravitational heating can hardly account for all the observations (e.g., Borgani et al. 2002), cooling in itself gives rise to the well know overcooling problem, i.e., a too large fraction of ICM converted into a cold "stellar" phase (Balogh et al. 2001; Tornatore et al. 2003).

In the first part of this contribution, I will discuss how the evolution of the cluster population can be used to place constraints on cosmology, and the level of uncertainty in the determination of cosmological parameters, which is associated with the uncertainty in the knowledge of the ICM properties. In the second part I will show examples of how large hydrodynamical simulations of galaxy clusters and groups can be used to make progress in the description of the ICM physics.

2. Cosmology with Galaxy Clusters

The mass distribution of dark matter halos undergoing spherical collapse in the framework of hierarchical clustering is described by the Press-Schechter distribution (PS, Press &Schechter 1974). The number of such halos in the mass range $[M, M+dM]$ can be written as $n(M,z)dM = \bar{\rho}\, M\, f(\nu)\, (d\nu/dM)\, dM$ where $\bar{\rho}$ is the cosmic mean density. The function f depends only on the variable $\nu = \delta_c(z)/\sigma_M$. $\delta_c(z)$ is the linear-theory overdensity extrapolated to the present time for a uniform spherical fluctuation collapsing at redshift z, which depends on cosmology through the growth factor for linear density fluctuations ($\delta_c = 1.68(1+z)$ for an Einstein-de Sitter cosmology). The r.m.s. density fluctuation at the mass scale M, σ_M, is connected to the fluctuation power spectrum, $P(k)$, whose normalization is usually expressed in terms of σ_8, the r.m.s. density fluctuation within a top-hat sphere of $8\,h^{-1}$Mpc radius.

In their original derivation of the cosmological mass function, Press & Schechter (1974) obtained the expression $f(\nu) = (2\pi)^{-1/2}\exp(-\nu^2/2)$ for Gaussian density fluctuations. Despite its subtle simplicity, the PS mass function has served for more than a decade as a guide to constrain cosmological parameters from the mass function of galaxy clusters. Only with the advent of the last generation of N-body simulations, which are able to span a very large dynamical range, significant deviations of the PS expression from the exact numerical description of gravitational clustering have been noticed (e.g., Jenkins et al. 2001, Evrard et al. 2002; White 2002). Such deviations are interpreted in terms of corrections to the PS approach, e.g., by incorporating the effects of non-spherical collapse (Sheth & Tormen 1999). I show in Figure 1 how the mass function can be used to constrain cosmological models. In the left panel I show that, for a fixed value of the observed cluster mass function, the implied value of σ_8 increases as the density parameter decreases. Determinations of the cluster mass function in the local Universe using a variety of samples and methods indicate that $\sigma_8\Omega_m^\alpha = 0.4-0.6$, where $\alpha \simeq 0.4-0.6$, almost independent of the presence of a cosmological constant term providing spatial flatness (e.g., Reiprich & Böhringer 2001; Ikebe et al. 2002; Pierpaoli et al. 2003, and references therein).

The growth rate of the density perturbations depends primarily on Ω_m and, to a lesser extent, on Ω_Λ, at least out to $z \sim 1$, where the evolution of the cluster population is currently studied. Therefore, following the evolution of the cluster space density over a large redshift baseline, one can break the degeneracy between σ_8 and Ω_m. This is shown in the right panel of Figure 1: models with different values of Ω_m, which are normalized to yield the same number density of nearby clusters, predict cumulative mass functions that progressively differ by up to orders of magnitude at increasing redshifts.

A commonly adopted procedure to estimate cluster masses is based on the measurement of the temperature of the ICM. Based on the assumption that gas and dark matter particles share the same dynamics within the cluster potential well, the temperature T and the velocity dispersion σ_v are connected by the relation $k_BT = \beta\mu m_p\sigma_v^2$, where $\beta = 1$ would correspond to the case of a perfectly thermalized gas. If we assume spherical symmetry, hydrostatic equilibrium and isothermality of the gas, the solution of the equation of hydrostatic equilibrium provides the link between the total cluster virial mass, $M_{\rm vir}$, and the ICM temperature: $k_BT \propto \beta^{-1}M_{\rm vir}^{2/3}[\Omega_m\Delta_{vir}(z)]^{1/3}(1+z)\,{\rm keV}$, where $\Delta_{vir}(z)$ is the ratio between the average density within the virial radius and the mean cosmic density at redshift z. The above expression for the M–T relation is fairly consistent with hydrodynamical cluster simulations with $0.9 \lesssim \beta \lesssim 1.3$ (e.g., Bryan & Norman 1998, Frenk et al. 1999). Observational data on the $M_{\rm vir}$–T relation show consistency with the $T \propto M_{\rm vir}^{2/3}$ scaling law, at least for $T \gtrsim 3$ keV clusters, but with a $\sim 40\%$ lower normaliza-

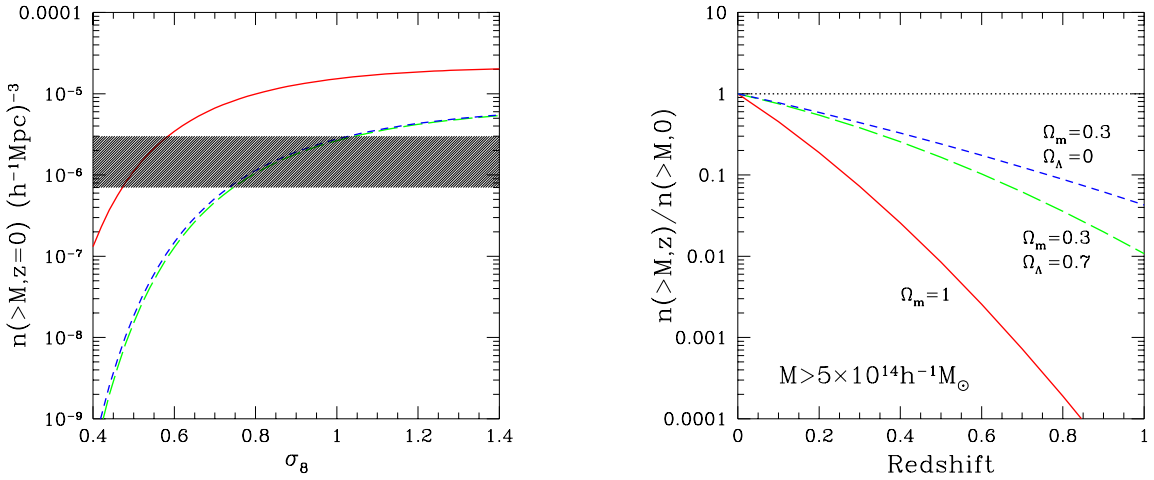

FIG. 1.— The sensitivity of the cluster mass function to cosmological models. Left: the cumulative mass function at $z = 0$ for $M > 5 \times 10^{14} h^{-1} M_\odot$ for three cosmologies, as a function of σ_8, with shape parameter $\Gamma = 0.2$; solid line: $\Omega_m = 1$; short-dashed line: $\Omega_m = 0.3$, $\Omega_\Lambda = 0.7$; long-dashed line: $\Omega_m = 0.3$, $\Omega_\Lambda = 0$. The shaded area indicates the observational uncertainty in the determination of the local cluster space density. Right: Evolution of $n(>M, z)$ for the same cosmologies and the same mass-limit, with $\sigma_8 = 0.5$ for the $\Omega_m = 1$ case and $\sigma_8 = 0.8$ for the low-density models.

tion (e.g., Finoguenov et al. 2001). We will discuss in the next section possible reasons for this difference between the observed and the simulated M–T relation. In any case, such uncertainties in the correct value of the normalization of the M–T relation translates into an uncertain determination of σ_8 (for a fixed value of Ω_m): the higher this normalization, the larger the mass corresponding to a given temperature, the larger the value of σ_8 required for the predicted mass function to match the observed X-ray temperature function (XTF; e.g., Pierpaoli et al. 2003; Seljak et al. 2002). In Figure 2 we show the analysis by Pierpaoli et al. (2003), who quantified the change in σ_8 (for $\Omega_m = 0.3$) induced by varying the M–T normalization.

Another method to trace the evolution of the cluster number density is based on the XLF. The advantage of using X-ray luminosity as a tracer of the mass is that L_X is measured for a much larger number of clusters within samples with well-defined selection properties. The most recent flux-limited cluster samples contain now a large (~ 100) number of objects, which are homogeneously identified over a broad redshift baseline, out to $z \simeq 1.3$. A useful parameterization for the relation between temperature and bolometric luminosity is $L_{bol} \propto T_X^\alpha (1+z)^A (d_L(z)/d_{L,EdS}(z))^2$, with $d_L(z)$ the luminosity-distance at redshift z for a given cosmology. Independent analyses of nearby clusters with $T_X \gtrsim 2$ keV consistently show that $\alpha \simeq 2.5$–3 (e.g., Arnaud & Evrard 1999 and references therein), with no evidence for a strong evolution out to $z \gtrsim 1$ (e.g., Ettori et al. 2003; cf. also Vikhlinin et al. 2002).

In Figure 3 we show the constraints on the σ_8–Ω_m plane obtained from the ROSAT Deep Cluster Survey (Borgani et al. 2001; Rosati et al. 2002). The different panels report the effect of changing in different ways

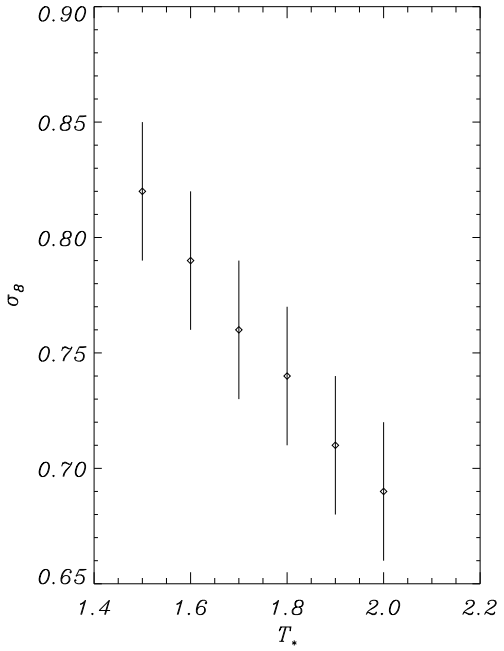

FIG. 2.— The dependence of σ_8 on the value of the M–T normalization. Here the density parameter is fixed at $\Omega_m = 0.3$ (from Pierpaoli et al. 2003).

the parameters defining the M–L_X relation, such as the slope α and the evolution A of the L_X–T relation, the normalization β of the M–T relation, and the overall scatter Δ_{M-L_X}. Figure 3 demonstrates that firm conclusions about the value of the matter density parameter Ω_m can be drawn from available samples of X-ray

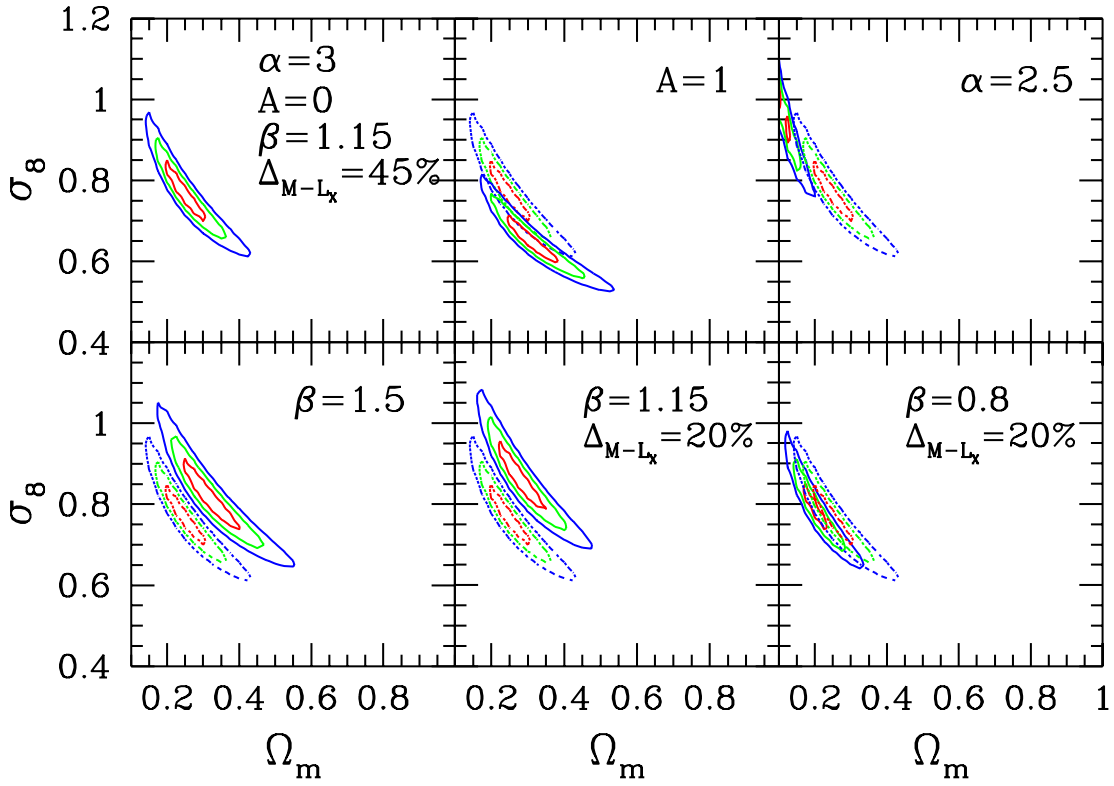

FIG. 3.— Probability contours in the σ_8–Ω_m plane from the evolution of the X-ray luminosity distribution of RDCS clusters. Different panels refer to different ways of changing the relation between cluster virial mass, M, and X-ray luminosity, L_X, within theoretical and observational uncertainties. The upper left panel shows the analysis corresponding to the choice of a reference parameter set. In each panel, we indicate the parameters which are varied, with the dotted contours always showing the reference analysis.

clusters. In keeping with most of the analyses in the literature, based on independent methods, a critical density model cannot be reconciled with data. Specifically, $\Omega_m < 0.5$ at 3σ level even within the full range of current uncertainties in the relation between mass and X-ray luminosity. However, the results shown in Fig. 3 also demonstrate that constraints in the σ_8–Ω_m may change by changing the M–L_X relation within current uncertainties, by an amount which is at least as large as the statistical uncertainties. This emphasizes that the main obstacle toward a precision estimate of cosmological parameter with forthcoming large cluster surveys will lie in the systematic uncertainties in our description of the ICM properties, rather than in the limited statistics of distant clusters.

3. Hydrodynamical Simulations of Clusters

In this section I present results from a large cosmological hydrodynamical simulation of a concordance ΛCDM model ($\Omega_m = 1 - \Omega_\Lambda = 0.3$, $\Omega_{bar} = 0.04$, $h = 0.7$, $\sigma_8 = 0.8$) within a box of $192\,h^{-1}$Mpc on a side, using 480^3 dark matter and an equal number of gas particles, and a Plummer-equivalent softening for the computation of the gravitational force of $7.5h^{-1}$kpc (Borgani et al. 2003). The run has been realized using GADGET[1], a massively parallel tree N-body/SPH code (Springel, Yoshida & White 2001), which treats radiative cooling, star formation from a multiphase ISM and the effect of galactic winds (Springel & Hernquist 2003). With such characteristics, our simulation has enough resolution to allow reliable estimates of the ICM properties, while allowing to simulate at once a fairly large cosmological volume.

In the left panel of Figure 4, we show a map of the gas distribution at $z = 0$. The panel on the right shows the gas distribution around the most massive cluster found in the simulation and represents a zoom-in of the whole simulation box by about a factor of 20. The amount of small-scale detail which is visible in the zoom-in of the right panel demonstrates the large dynamic range encompassed by the hydrodynamic treatment of the gas in our simulation.

As shown in Figure 5, the overall fraction of baryons found to be in stars in the whole simulation volume is $f_* \simeq 7$ per cent, thus consistent with observational results (e.g., Balogh et al. 2001). At the same time, the efficiency of star formation within the high-density environment of clusters is still in excess with respect to observations. Values of f_* for individual clusters are at the level of $\simeq 20$ per cent for $T > 3$ keV clusters, with a slight tendency to increase for colder systems, as shown in Figure 5. Therefore, the efficiency of cooling and star

[1] `http://www.mpa-garching.mpg.de/gadget`

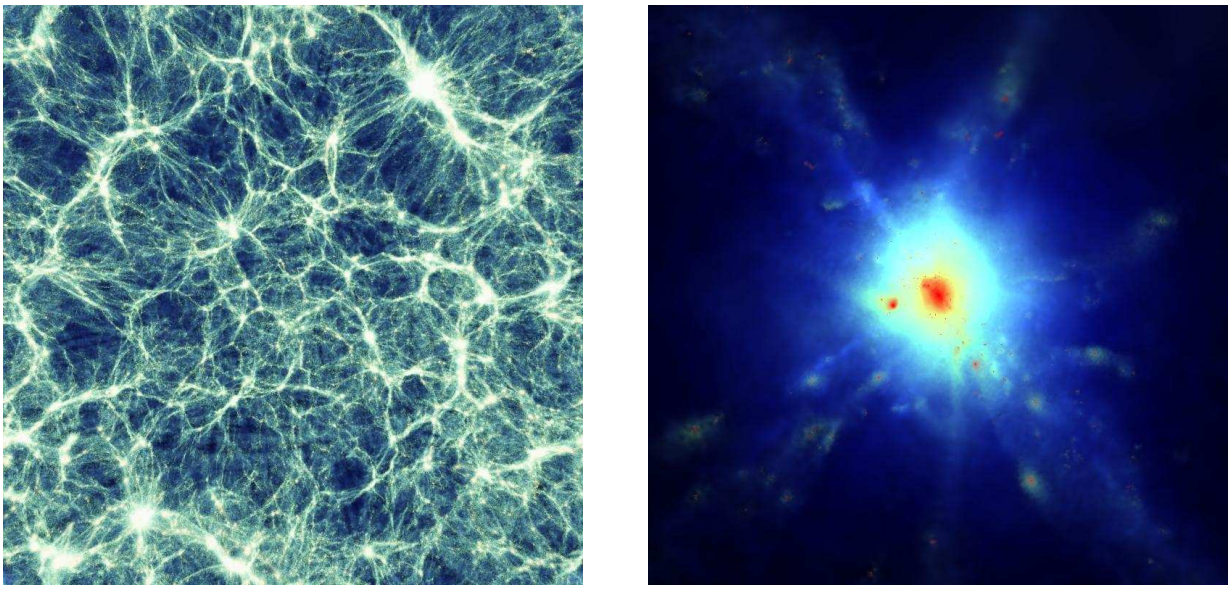

FIG. 4.— Left panel: map of the gas density over the whole simulation box at $z = 0$, projected through a slice having thickness of 12 h^{-1}Mpc, and containing the most massive cluster found in the simulation (upper right side of the panel). Right panel: zoom into the region of the largest cluster; the cluster is shown out to two virial radii.

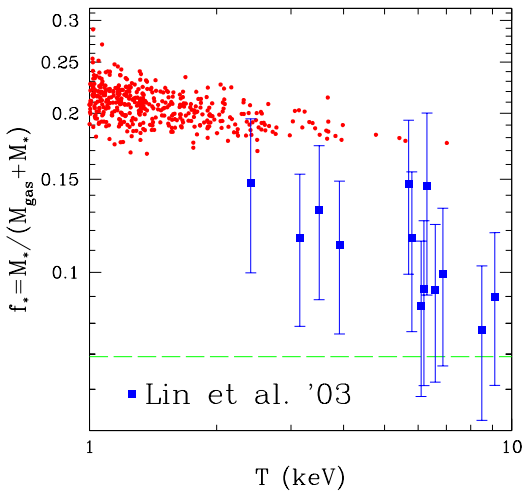

FIG. 5.— The fraction of gas locked into stars, estimated at the virial radius from simulations (small circles) and from observational data (big squares with errorbars; from Lin et al. 2003). The horizontal dashed line indicates the cosmic value of f_* found in the simulation.

formation in well resolved objects is still too high in our simulation.

We show in Figure 6 the comparison between the simulated and the observed M–T relation. The left panel demonstrates that cooling in our simulation is not effective in reducing the M–T normalization to the observed level. In this panel, our results are compared to those by Finoguenov et al. (2001). Making a log–log least square fitting to the relation $\log(M_{500}/M_0) = \alpha \log(T_{500}/\mathrm{keV})$, we obtain $\alpha = 1.59 \pm 0.05$ and $M_0 = (2.5 \pm 0.1)\, 10^{13} h^{-1} M_\odot$. Therefore, the normalization of our relation at 1 keV turns out to be higher by about 20 per cent than the observed one. The intrinsic scatter around the best-fitting relation is $\Delta M/M = 0.16$.

A critical issue in this comparison concerns the different procedure used for estimating masses in simulations and in observations. For instance, Finoguenov et al. (2001) estimate masses by applying the equation of hydrostatic equilibrium, assuming a β-model for the gas density profile and a polytropic equation of state of the form $T \propto \rho_{\rm gas}^{\gamma-1}$. In order to verify whether such a procedure leads to a biased estimate of cluster masses, we follow this same procedure to estimate masses of simulated clusters. For each cluster, we fit the gas density profile to the β-model, while temperature and gas-density profiles are fitted to a polytropic equation of state. As shown in Figure 7, the effect of using such a mass estimator is that of lowering the normalization of the M–T relation and to bring it into better agreement with observations.

Allen et al. (2001) used Chandra data to resolve temperature profiles for hot relaxed clusters and avoided the assumption of a β-model for the gas density profile. In this way, the resulting M–T relation from their analysis can be directly compared to the simulation result based on the "true" cluster masses. The resulting best-fitting M_{2500}–T_{2500} relation is plotted as a dashed line in the right panel of Fig. 6 and compared to the results of our simulation. It is quite remarkable that the simulation results now agree with observations on the M–T relation. Still, this result suggests that observed and simulated M–T relations agree with each other when high-quality observational data are used which accurately resolves the surface-brightness profile and the temperature structure of clusters. Thanks to the good statistics offered by our simulation, a reliable calibration of the scatter expected in the M–T relation can be obtained. We suggest that this calibration should be used for the determination of

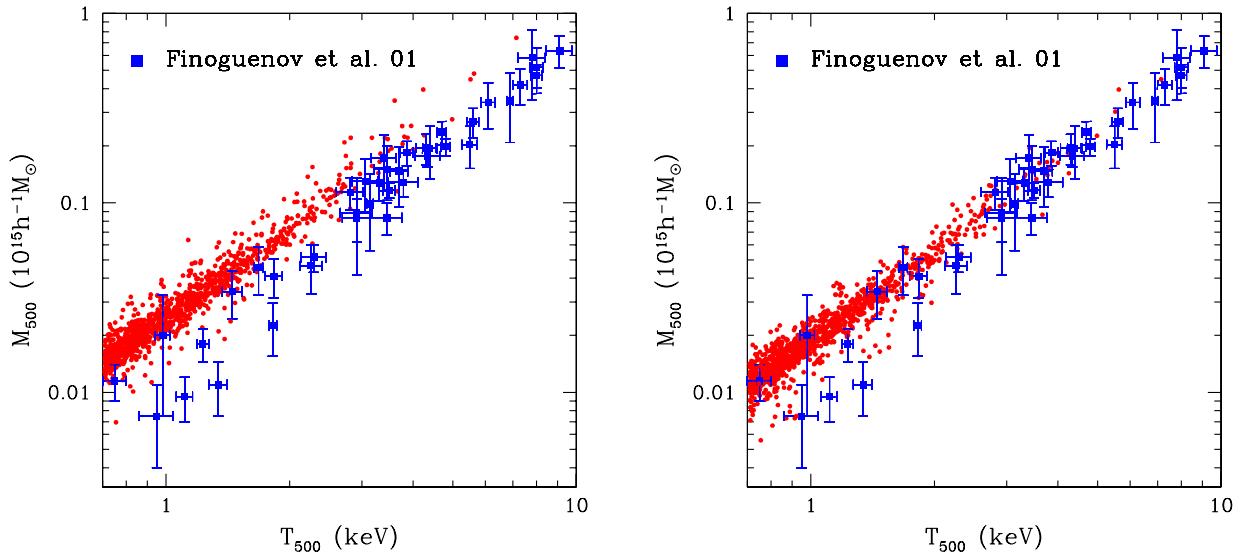

FIG. 6.— Comparison between the observed and the simulated M–T relation. Left and right panels refer to the relation at $\bar{\rho}/\rho_c = 500$. In the left panel we compare the results from Finoguenov et al. (2001) to the true total masses of simulated clusters. In the right panel, cluster masses are estimated by assuming a β-model and a polytropic equation of state in the solution of the equation of hydrostatic equilibrium.

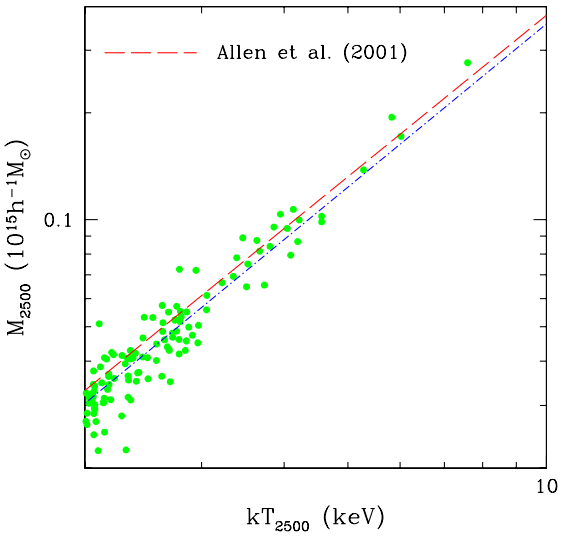

FIG. 7.— The simulation results for the M–T relation at $\bar{\rho}/\rho_c = 2500$ are compared to the relation found by Allen et al. (2001) from Chandra for hot relaxed clusters (dashed line); the dot-dashed line is our best-fit to the clusters with $T_{2500} > 2$ keV.

cosmological parameters from the XTF and XLF. This shows the importance of a precise calibration of the relations between theory-predicted mass and X-ray observed quantities, and highlights the important role that large cosmological simulations can play in understanding the systematics involved.

As for the temperature profiles, observational data from the ASCA (e.g., Markevitch et al. 1998), BeppoSAX (De Grandi & Molendi 2002) and XMM-Newton (e.g., Pratt & Arnaud 2002) satellites show that temperature profiles decline at cluster-centric distances larger than about one quarter of the virial radius. Furthermore, Allen et al. (2001) analysed Chandra data for 6 fairly relaxed hot clusters, with $T \gtrsim 5.5$ keV. They found profiles which are quite similar once they are rescaled to R_{2500}: an isothermal profile in the range $0.3 \lesssim /R_{2500} \lesssim 1$, with a smooth decline at smaller radii. While a declining profile in the outer cluster regions is expected from hydrodynamical simulations, the presence of a nearly isothermal core with a central smooth temperature drop represents a non-trivial challenge for numerical models of the ICM (e.g., Tornatore et al. 2003). If any, cooling generates a lack of pressure support in central regions, which causes gas infall from outer regions, and this gas is heated by adiabatic compression as it streams toward the centre. Overall, in the presence of cooling, the gas temperature increases at the center, thus leading to a steepening of the temperature profiles.

We show in Figure 8 a comparison between observed and simulated T-profiles. For a proper comparison with the results by De Grandi & Molendi (2002), we select only clusters with $T > 3$ keV, which is the range covered by their 17 clusters observed with BeppoSAX. After projection, the average profile of the simulated clusters does still not show evidence for an isothermal core. As a consequence, once normalized to the emission-weighted temperature, the simulation profile is higher in central regions and lower at $R \gtrsim 0.1R_{180}$ when compared to an equivalent observed system. To further demonstrate the failure of the simulation to account for the observed central temperature profiles, we compare our results in the right panel of Fig. 8 to those obtained by Allen et al. (2001). Again, the observed universal profile by Allen et al. largely deviates from the simulated one. We argue that this discrepancy between simulated and observed temperature profiles is strong evidence for the current lack of a self-consistent simulation model capable of explaining the thermal structure of the ICM in the regime where radiative cooling and feedback heating are highly important.

Gas entropy is currently receiving considerable atten-

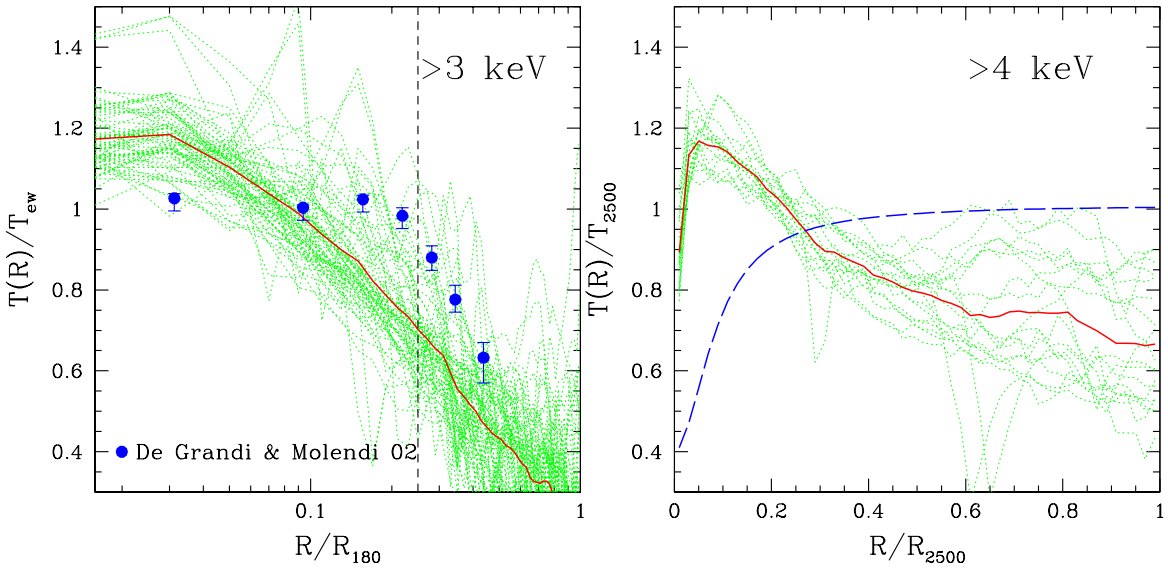

FIG. 8.— Comparison between simulated and observed projected temperature profiles. Left panel: comparison between simulated clusters with $T_{\rm ew} > 3$ keV and the observational data points from the analysis of BeppoSAX data for 17 clusters by De Grandi & Molendi (2002); projected radial scales are in units of R_{180}, i.e. the radius at which $\bar{\rho}/\rho_{\rm cr} = 180$. Right panel: comparison between simulated clusters with $T_{\rm ew} > 4$ keV and the best-fitting universal temperature profiles measured by Allen et al. (2001) from their analysis of Chandra data for a set of six relaxed clusters (dashed curve); projected radial scales are in units of R_{2500}. In both panels, dotted lines are the profiles for each single simulated cluster, while the heavy solid line is for the average profile. For reference, the vertical dashed line in the left panel indicates the average value of R_{2500}.

tion as a diagnostic tool for tracing the past dynamical and thermal history of the ICM (e.g., Ponman et al. 1999; Tozzi & Norman 2001; Balogh et al. 2001; Voit et al. 2002). In X-ray studies of galaxy clusters, the "entropy" is commonly defined as $S = \frac{T}{n_e^{2/3}}$, where n_e is the electron number density. As long as the gas adiabat is not altered by some non-gravitational heating source, one can derive the expected scaling between entropy and temperature in the form $S \propto T$. When going from rich clusters to poor groups, we probe gas that has been accreted at higher redshift, when it was harder to generate accretion shocks and, therefore, to increase the gas entropy. For this reason, the entropy excess measured in the central regions of poor clusters and groups is considered to provide direct evidence that some non-gravitational process must have modified the gas adiabat. Models based on an entropy floor (e.g., Tozzi & Norman 2001) or on cooling (e.g., Voit et al. 2002) have been proposed to account for the lack of self-similarity in central cluster regions.

As shown in Figure 9, the clusters from our simulation, which includes both cooling and SN feedback, show an excess of entropy with respect to the prediction of self-similar scaling. However, such an excess is not enough to match the recent observational data on the "entropy ramp" by Ponman et al. (2003). This result suggests that the adopted recipe for supernova feedback from the stellar population is not strong enough to increase the gas adiabat in central cluster regions. At the same time, radiative cooling is not able by itself to break the self-similarity of the ICM entropy structure as strongly as observed. Furthermore, since our simulation does not follow in a self-consistent way the production of metals, we have assumed a zero-metallicity cooling function. Including metals would increase the cooling efficiency and, therefore, the limiting entropy for the removal of gas from central cluster regions. This suggests that a proper treatment of the ICM metal enrichment is also required to make a close comparison with observational data on the entropy excess in groups.

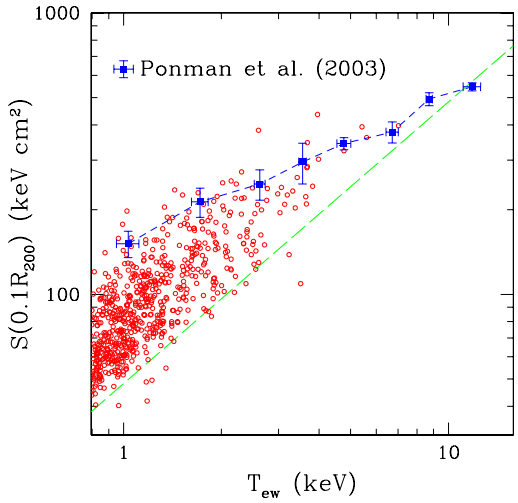

FIG. 9.— The relation between gas entropy computed at $0.1\,r_{\rm vir}$ and $T_{\rm ew}$. Data points are taken from Ponman et al. (2003). The dashed line shows for reference the self-similar scaling $S \propto T$, normalized to the hottest cluster found in the simulation.

4. **Discussion**

The analysis presented here, aimed at using galaxy clusters as tools to measure cosmological parameters,

demonstrates that they can indeed be used to trace the past dynamical history of the Universe and, therefore, to measure the density parameter and the amplitude and shape of the power spectrum of density perturbations. While this represents the optimistic point of view of the results presented, the pessimistic view would be that uncertainties in the relation between cluster collapsed mass and X-ray observable quantities still prevent such constraints to reach a precision better than about 20 per cent. Such systematic uncertainties have been shown to be comparable, if not larger, than those associated to statistics, i.e. to the limited number of clusters known at high redshift.

This calls for the need of a better observational calibration of the mass–luminosity and mass–temperature relations, and for an improved understanding of the physical mechanisms which determine the thermodynamical properties of the ICM. There is no doubt that a significant progress of our understanding of the physical processes taking place in the ICM is mandatory if galaxy clusters have to take part to the so-called era of precision cosmology.

In the second part of this contribution I have discussed how hydrodynamical simulations of clusters in cosmological context represent an invaluable instrument to investigate the role that astrophysical processes, such as shocks, cooling, star formation, SN and AGN feedback, play in determining the ICM observational properties. The results presented here show that the physical processes included in our simulation are able to account for the basic global properties of clusters, such as the scaling relations between mass and temperature. At the same time, we find indications suggesting that a more efficient way of providing non-gravitational heating from feedback energy compared to what is implemented in the simulation is required: this "extra heating" should not only reduce the amount of gas that cools, but also needs to "soften" the gas density profiles of poor clusters and groups by increasing the ICM entropy. Other sources of energy appear therefore as increasingly attractive possibilities, for example SN-Ia. The energetics of SN-Ia is usually considered to be subdominant, otherwise they would produce too much Iron and overpollute the ICM (e.g., Renzini 1997; Pipino et al. 2002). On the other hand, because the progenitors of SN-Ia have a much longer life-time than those of SN-II, the corresponding energy is released more gradually into a medium which is already heated by the shorter-lived SN-II. This heated gas has hence already a longer cooling time, making SN-Ia potentially a much more efficient heating source than SN-II. A further source of energy feedback, which is not included in our simulation, is represented by AGN. Theoretical calculations show that a fractional coupling of the energy released by the AGN with the surrounding ICM at the level of $f \approx 0.01$ would be sufficient to account for the L_X–T relations of groups (Cavaliere, Lapi & Menci 2002). While a number of hydrodynamical cosmological codes now include a treatment for star formation and SN feedback, none of them includes yet a self-consistent treatment of energy release from AGN.

Perhaps the most puzzling discrepancy with observations concerns the temperature profiles. Cooling causes a lack of pressure support in the cluster center, causing gas to flow in from outer regions, thus being heated by adiabatic compression (e.g., Tornatore et al. 2003). As a result, the temperature actually increases in cooling regions, causing steeply increasing temperature profiles. This picture is quite discrepant compared to the standard cooling-flow model, where a population of gas particles at very low temperature should be detected (see Fabian 1994, for a review). Even more importantly, it also conflicts with the observational picture emerging from Chandra and XMM-Newton observations: the ICM in cluster central regions has temperatures between 1/2 and 1/4 of the virial temperature, with no signature for the presence of colder gas (e.g., Peterson et al. 2001). It is this gas, which is not allowed to cool below that temperature and drop out of the hot phase, that causes the smooth decrease of the central temperature profiles. In fact, observations point now toward a quite small rate of cooling in central cluster regions, with mass-deposition rates reduced by a factor 5–10 with respect to pre-Chandra/XMM observations (e.g., Blanton, Sarazin & McNamara 2003).

In the light of this discussion, it is clear that the challenge for numerical simulations of cluster formation has shifted from problems related to resolution and dynamic range to those concerned with the proper treatment of the complex physical processes which determine the thermal state of cosmic baryons. The simulation presented here demonstrates that code efficiency and super-computing capabilities make it possible to describe cosmic structure formation over a fairly large dynamic range. With the ever growing super-computing power, the real challenge for numerical cosmology in the coming years will then be to construct algorithms that more faithfully incorporate all those additional astrophysical processes that apparently are crucial for understanding the observational properties of galaxies and clusters of galaxies.

The simulation presented here has been realized using the IBM-SP4 machine at the "Centro Interuniversitario del Nord-Est per il Calcolo Elettronico" (CINECA, Bologna), with CPU time assigned thanks to an INAF-CINECA grant. I would like to thank all the people who collaborated with me on the results presented in this paper. In alphabetic order, they are: Antonaldo Diaferio, Klaus Dolag, Lauro Moscardini, Giuseppe Murante, Colin Norman, Elena Pierpaoli, Piero Rosati, Douglas Scott, Volker Springel, Giuseppe Tormen, Luca Tornatore, Paolo Tozzi and Martin White.

References

Allen, S. W., Schmidt, R. W., & Fabian, A. C. 2001, MNRAS, 328, L37

Arnaud, M. & Evrard, A. E. 1999, MNRAS, 305, 631

Balogh, M. L., Pearce, F. R., Bower, R. G., & Kay, S. T. 2001, MNRAS, 326, 1228
Blanton, E. L., Sarazin, C. L., & McNamara, B. R. 2003, ApJ, 585, 227
Borgani, S. et al. 2001, ApJ, 561, 13
Borgani, S., Governato, F., Wadsley, J., Menci, N., Tozzi, P., Quinn, T., Stadel, J., & Lake, G. 2002, MNRAS, 336, 409
Borgani, S., Murante, G., Springel, V., et al. 2003, MNRAS, submitted
Bryan, G. L. & Norman, M. L. 1998, ApJ, 495, 80
Cavaliere, A., Lapi, A., & Menci, N. 2002, ApJ, 581, L1
De Grandi, S. & Molendi, S. 2002, ApJ, 567, 163
Eke, V. R., Cole, S., Frenk, C. S., & Patrick Henry, J. 1998, MNRAS, 298, 1145
Ettori, S., Tozzi, P., Borgani, S., & Rosati, P. 2003, A&A, submitted
Evrard, A. E. et al. 2002, ApJ, 573, 7
Fabian, A. C. 1994, ARA&A, 32, 277
Finoguenov, A., Reiprich, T. H., & Böhringer, H. 2001, A&A, 368, 749
Frenk, C. S. et al. 1999, ApJ, 525, 554
Ikebe, Y., Reiprich, T. H., Böhringer, H., Tanaka, Y., & Kitayama, T. 2002, A&A, 383, 773
Jenkins, A., Frenk, C. S., White, S. D. M., Colberg, J. M., Cole, S., Evrard, A. E., Couchman, H. M. P., & Yoshida, N. 2001, MNRAS, 321, 372
Kaiser, N. 1986, MNRAS, 222, 323
Lin, Y., Mohr, J. J., & Stanford, S. A. 2003, ApJ, 591, 749
Markevitch, M., Forman, W. R., Sarazin, C. L., & Vikhlinin, A. 1998, ApJ, 503, 77
Oukbir, J. & Blanchard, A. 1992, A&A, 262, L21
Peterson, J. R. et al. 2001, A&A, 365, L104
Pierpaoli, E., Borgani, S., Scott, D., & White, M. 2003, MNRAS, 342, 163
Pipino, A., Matteucci, F., Borgani, S., & Biviano, A. 2002, New Astronomy, 7, 227
Ponman, T. J., Cannon, D. B., & Navarro, J. F. 1999, Nature, 397, 135
Ponman, T. J., Sanderson, A. J. R., & Finoguenov, A. 2003, MNRAS, 343, 331
Pratt, G. W. & Arnaud, M. 2002, A&A, 394, 375
Press, W. H. & Schechter, P. 1974, ApJ, 187, 425
Reiprich, T. H. & Böhringer, H. 2002, ApJ, 567, 716
Renzini, A. 1997, ApJ, 488, 35
Rosati, P., Borgani, S., & Norman, C. 2002, ARA&A, 40, 539
Sanderson, A. J. R., Ponman, T. J., Finoguenov, A., Lloyd-Davies, E. J., & Markevitch, M. 2003, MNRAS, 340, 989
Seljak, U. 2002, MNRAS, 337, 769
Sheth, R. K. & Tormen, G. 1999, MNRAS, 308, 119
Spergel, D. N. et al. 2003, ApJS, 148, 175
Springel, V. & Hernquist, L. 2003, MNRAS, 339, 289
Springel, V., Yoshida, N., & White, S. D. M. 2001, New Astronomy, 6, 79
Tornatore, L., Borgani, S., Springel, V., Matteucci, F., Menci, N., & Murante, G. 2003, MNRAS, 342, 1025
Tozzi, P. & Norman, C. 2001, ApJ, 546, 63
Vikhlinin, A., VanSpeybroeck, L., Markevitch, M., Forman, W. R., & Grego, L. 2002, ApJ, 578, L107
Voit, G. M., Bryan, G. L., Balogh, M. L., & Bower, R. G. 2002, ApJ, 576, 601
White, M. 2002, ApJS, 143, 241